



Published in final edited form as:

Mol Cell. 2015 August 20; 59(4): 639–650. doi:10.1016/j.molcel.2015.06.027.

Repression of the heat shock response is a programmed event at the onset of reproduction

Johnathan Labbadia and Richard I Morimoto¹

Department of Molecular Biosciences, Rice Institute for Biomedical Research Northwestern University, Evanston, IL, USA

Summary

The heat shock response (HSR) is essential for proteostasis and cellular health. In metazoans, aging is associated with a decline in quality control, thus increasing the risk for protein conformational disease. Here, we show that in *C. elegans*, the HSR declines precipitously over a four hour period in early adulthood coincident with the onset of reproductive maturity. Repression of the HSR occurs due to an increase in H3K27me3 marks at stress gene loci, the timing of which is determined by reduced expression of the H3K27 demethylase *jmjd-3.1*. This results in a repressed chromatin state that interferes with HSF-1 binding and suppresses transcription initiation in response to stress. The removal of germ line stem cells preserves *jmjd-3.1* expression, suppresses the accumulation of H3K27me3 at stress gene loci and maintains the HSR. These findings suggest that competing requirements of the germ line and soma dictate organismal stress resistance as animals begin reproduction.

Introduction

The ability to maintain protein homeostasis (proteostasis) is a prerequisite for proper cellular function and is achieved through the proteostasis network (PN) (Labbadia and Morimoto, 2015). Molecular chaperones, protein degradation pathways and the translational machinery form the core of the PN and are precisely coordinated to ensure that rates of protein synthesis, folding and degradation are balanced to meet the ever changing demands placed upon the proteome (Labbadia and Morimoto, 2015).

Although the PN is thought to be robust, exposure to environmental or physiological stress or expression of mutant proteins challenges the PN, leading to an accumulation of misfolded proteins, toxic oligomers and protein aggregates (Labbadia and Morimoto, 2015). To combat this, cells have evolved multiple cell stress response pathways including the heat

¹Correspondence to: Department of Molecular Biosciences Rice Institute for Biomedical Research Northwestern University 2205 Tech Drive, Hogan 2-100, Evanston, IL 60208, USA Phone: 847-491-3340 Fax: 847-491-4461 r-morimoto@northwestern.edu.

Publisher's Disclaimer: This is a PDF file of an unedited manuscript that has been accepted for publication. As a service to our customers we are providing this early version of the manuscript. The manuscript will undergo copyediting, typesetting, and review of the resulting proof before it is published in its final citable form. Please note that during the production process errors may be discovered which could affect the content, and all legal disclaimers that apply to the journal pertain.

Author contributions

J.L. designed and performed experiments, analyzed data and constructed figures. R.I.M designed experiments and analyzed data. J.L. and R.I.M wrote the manuscript.

shock response (HSR), the organellar unfolded protein responses (UPRs), and the antioxidant stress response, which rapidly up-regulate molecular chaperones and detoxification enzymes to diminish the consequences of protein damage across cellular compartments (Akerfelt et al., 2010; Haynes et al., 2013; Sykietis and Bohmann, 2010; Walter and Ron, 2011). Cell stress response pathways confer malleability to the PN and are essential for cells to properly buffer against protein misfolding in the face of environmental insults and demanding physiological processes such as growth, development and differentiation (Morimoto, 2008). As such, stress response pathways are intimately coupled with organismal health and must be regulated with exquisite precision to ensure that the timing, magnitude and duration of gene induction are proportional to the stress encountered and the extent of protein misfolding (Morimoto, 2008).

The PN, stress responses, aging and disease are inextricably linked (Henis-Korenblit et al., 2010; Hsu et al., 2003; Morley and Morimoto, 2004; Rea et al., 2005; Shore et al., 2012; Taylor and Dillin, 2013; Tullet et al., 2008). In *Caenorhabditis elegans*, protein misfolding and aggregation can be detected under normal growth conditions in multiple tissues in early adulthood, well before the onset of gross age-related morphological and behavioral changes (Ben-Zvi et al., 2009; David et al., 2010; Reis-Rodrigues et al., 2012). This coincides with a decline in the HSR and UPR^{ER}, suggesting that the collapse of stress response pathways may contribute to a loss of proteostasis early in life (Ben-Zvi et al., 2009; Taylor and Dillin, 2013). These observations reinforce the idea that dysregulation of stress response pathways and the accumulation of misfolded proteins could be a common aspect of diverse protein folding diseases (Huang et al., 2011; Labbadia et al., 2011; Olzscha et al., 2011). Despite this, remarkably little is known regarding the regulation of stress response pathways and stress resistance in metazoans as they proceed through life.

To address this, we examined how *C. elegans* responded to a battery of stressful conditions during early adulthood. We found that multiple stress responses become transcriptionally repressed on the first day of adulthood, resulting in animals that are much more susceptible to environmental stress. By focusing on the HSR, we found that transcriptional repression occurs within a 4 hour window and coincides with the onset of egg-laying, suggesting that interplay between the germ line and the soma results in active remodeling of stress responses once animals are committed to reproduce. Using a combination of genetic and biochemical approaches we found that the global repression of stress responses is controlled by signals from germ line stem cells through the H3K27me3 demethylase *jmjd-3.1*, indicating that stress response collapse represents an active down-regulation of protective pathways at the onset of reproduction.

Results

The heat shock response declines abruptly in early adulthood

To determine when the HSR declines, we exposed *C. elegans* to heat shock (HS) at different days of adulthood and quantified the expression of canonical HSR genes. Regardless of maintenance temperature, the inducibility of the HSR declined by 60-80% between day 1 (defined here as 4 hours post L4) and day 2 (defined here as 28 hours post L4) of adulthood (Figures 1A, S1A and S1B) with a concomitant decline in the levels of HSP-16 following

heat shock in day 2 adults (Figure S1C and D). Repression of the HSR is not due to changes in the temperature threshold for maximal activation of the HSR (Figure S1E) or constitutive induction of HS genes at day 2 of adulthood (Figures S1F-H). Using a panel of temperature sensitive germ line mutants, we asked whether reduced induction of HS genes is a by-product of increased embryo mass during early adulthood. Removal of oocytes, sperm or the entire gonad did not influence collapse of the HSR between day 1 and day 2 of adulthood (Figures S1I-L), suggesting that increased embryo mass is not the root of HSR collapse.

To determine whether HS gene expression is simply delayed at day 2 of adulthood, we quantified the kinetics of *hsp-70* (*C12C8.1*) and *hsp-16.11* induction. At day 1 of adulthood, maximal levels of *hsp-70* and *hsp-16.11* mRNA were observed 1 hour post HS, with levels rapidly attenuating thereafter (Figures S2A and B). By comparison, maximal *hsp-70* and *hsp-16.11* mRNA levels in day 2 adults were 60% lower and peaked 2 hours post HS (Figures S2A and B). The attenuation of HS gene induction also occurred more slowly in day 2 adults, suggesting that both the maximal induction and kinetics of the HSR are significantly affected between day 1 and day 2 of adulthood (Figures S2A and B). Finally, to investigate whether changes in the HSR occur across the population and throughout the soma, we used transgenic animals expressing mCherry under the control of the *hsp-70* (*C12C8.1*) promoter. Robust reporter activation was observed in all animals following HS at day 1 of adulthood, whereas day 2 adults showed a pronounced decline in reporter activation across the soma and throughout the population (Figure S2C). Together, these results reveal that HSR decline is not gradual, but instead represents a precipitous collapse during the first 24 hours of adulthood.

Multiple stress response pathways are simultaneously repressed during early adulthood

To determine whether our observations extended to other stress response pathways, we exposed animals to specific chemical stressors that induce the endoplasmic reticulum UPR (UPR^{ER}), oxidative stress response (OxSR) and mitochondrial UPR (UPR^{mito}). The induction of each pathway following stress declined by 40-60% between day 1 and day 2 of adulthood and, in most instances, was independent of significant changes in basal gene expression (Figures 1B-D and S2D).

To determine whether the reduced activation of stress response pathways could have organismal consequences, we measured *C. elegans* survival at, and recovery from, elevated temperatures, and assayed resistance to paraquat or DTT treatment. Consistent with an impairment of stress response pathways, we found that the ability to resist all stress treatments was significantly reduced between day 1 and day 2 of adulthood (Figure 2A-D). These data reveal that a repression of multiple cell stress responses occurs as *C. elegans* traverse the first day of adulthood, resulting in reduced resistance to a battery of stresses early in adult life.

Repression of the HSR occurs within a 4 hour window on the first day of adulthood and marks the onset of reproduction

Our data indicate that the repression of cell stress responses is a feature of early adulthood in *C. elegans*. The first 24 hours of adulthood are accompanied by the cessation of sperm

production, opening of the vulva to the exterior, sperm activation and oocyte fertilization, early embryo development and egg-laying (Hirsh et al., 1976) (Figure 2E). To determine the precise timing of stress response decline during the first day of adulthood, we focused our attention on the HSR, the sensitivity and dynamic range of which are ideal for such studies. We found that the inducibility of the HSR is reduced by 60-70% between 8 and 12 hours into the first day of adulthood and coincides with the onset of egg-laying (Figure 2F and S2E). This suggests that repression of the HSR represents an actively controlled transcriptional re-tuning that marks the onset of reproductive maturity and could represent an early molecular event in the aging process. Furthermore, rapid repression of the HSR correlates with a dramatic impairment in the ability of animals to recover from acute heat shock (Figure 2G), suggesting that the transcriptional switch mid-way through the first day of adulthood has profound consequences for the organism. Moreover, maintaining *C. elegans* at slightly elevated ambient temperature (25°C) accelerates the onset of egg-laying on the first day of adulthood and results in earlier repression of the HSR (Figure S2F). Together, these data identify a precise time point in early adulthood when cell stress responses decline.

Impairment of the HSR occurs independently of gross changes in HSF-1 expression, localization or DNA binding activity

To understand the underlying mechanism of the HSR collapse, we focused our attention on the regulation of heat shock transcription factor HSF-1. The steps required for induction of the HSR by HSF-1 are well established (Akerfelt et al., 2010), allowing for a systematic interrogation of the pathway. Steady state mRNA levels of HSF-1 are unchanged during early adulthood, suggesting that altered HSF-1 expression does not underlie repression of the HSR (Figure 3A).

To exert effects on gene expression, HSF-1 must translocate to the nucleus and bind to heat shock elements (HSE) in target gene promoters (Akerfelt et al., 2010). Using *C. elegans* expressing a single integrated copy of HSF-1 C-terminally tagged with GFP, we found that consistent with previous reports (Morton and Lamitina, 2013; Tatum et al., 2015), HSF-1 is constitutively nuclear and forms foci upon heat shock (Figures 3B, S3A and B). However, no gross change in the levels of nuclear HSF-1 were observed at day 2 of adulthood (Figures 3B). We therefore reasoned that repression of the HSR is due to an inability of HSF-1 to engage with target promoters due to altered DNA binding activity at day 2 of adulthood. To test this, we used an established HSF-1 electrophoretic mobility assay to ask whether the ability of HSF-1 to bind to HSEs *ex vivo* is reduced at day 2 of adulthood. The ability of HSF-1 to bind to an oligonucleotide probe containing a mutated HSE was significantly reduced and the HSF-1::HSE complex could be competed away using an excess of cold probe, thereby confirming the specificity of our assay (Figure S3C). We found no measurable difference in the ability of HSF-1 to bind to an HSE under control or stress conditions at day 2 of adulthood (Figures 3C and D). These data suggest that HSR collapse is not due to a reduction in the levels, localization, trimerization or intrinsic DNA binding ability of HSF-1.

If HSF-1 is unaltered between day 1 and day 2 of adulthood, what is the basis for the decline in the HSR? To address this, we examined the *in vivo* occupancy of HSF-1 by chromatin immunoprecipitation coupled to qPCR (ChIP-qPCR) at specific HS gene loci (See Figure S3D for a schematic of the regions amplified following ChIP). The levels of HSF-1 at the *hsp-70* and *hsp-16.11* promoters increased approximately 2-fold following HS on day 1 of adulthood (Figures 3E and F), but not at the promoter of *cdc-42*, a gene that is not bound by HSF-1 and whose expression is unaffected by stress or age (Figure S3E) (Hoogewijs et al., 2008). In contrast, on day 2 of adulthood the association of HSF-1 with HS genes was reduced by 50% relative to day 1 adults (Figures 3E and F). Moreover, recruitment of RNA Polymerase II (RNA Pol-II) following heat shock was also impaired by 50-70% at HS loci in day 2 adults (Figures 3G and H) but unaffected at the *cdc-42* promoter which, as expected, exhibited no increase in Pol-II association in response to HS (Figure S3F). Relative to levels in day 1 adults, decreased levels of RNA Pol-II were detected at the promoter and gene body of *hsp-70* following stress, suggesting that transcriptional repression is primarily due to impaired transcription initiation (Figures 3G and I). Together, our data support a model in which the decline of the HSR in early adulthood is due to the reduced binding of HSF-1 upon stress, thereby affecting recruitment of RNA Pol-II and transcription initiation.

Impaired binding of HSF-1 to target promoters correlates with hallmarks of transcriptional repression

We reasoned that the most likely interpretation of our results was that reduced HSF-1 binding occurs *in vivo* due to altered chromatin accessibility. To address this, we monitored DNase I sensitivity, histone methylation and histone acetylation at the *hsp-70* promoter using gonad-less animals (*gon-2*) that still exhibit HSR decline between day 1 and day 2 of adulthood (Figure S1L). This approach allowed us to assess chromatin related changes in the soma without possible confounding effects from germ line nuclei. Our DNase I digestion conditions allowed us to identify regulatory elements within the *hsp-70* promoter, thereby confirming the sensitivity of the assay to differentiate between open and closed regions of chromatin (Figure S4A). Relative to day 1 adults, DNase I digestion of chromatin from day 2 adults was reduced by 50-70% across the *hsp-70* promoter and into the gene body (Figure 4A). Likewise DNase I digestion was also reduced at the *hsp-16.11* promoter, but not at the *cdc-42* promoter (Figure 4A).

To determine whether changes in histone marks could contribute to transcriptional repression at day 2, we used antibodies against specific marks of transcriptional activation or repression (Egelhofer et al., 2011) to perform ChIP-qPCR. We found no significant change in H3K9me3, H3K4me3, H4K8ac, H4K16ac or H4tetra-ac at the *hsp-70* locus in early adulthood (Figures S4B and C). However, levels of the repressive mark, H3K27me3 (Voigt et al., 2013), increased 2 to 3-fold at both *hsp-70* and *hsp-16.11* in day 2 adults (Figure 4B). Levels of H3K27me3 associated with the *cdc-42* promoter did not change and were found to be significantly lower than at the *hsp-70* or *hsp-16.11* promoters, consistent with the higher basal expression levels of this gene (Figure 4B). These chromatin changes extended to other stress gene loci as the levels of H3K27me3 were also significantly elevated 1.5 to 2-fold at

genes induced as part of the UPR^{ER} (*hsp-4*), UPR^{mito} (*hsp-6*) and OxSR (*gcs-1*) (Figure 4C).

These data indicate that at day 2 of adulthood, the promoter regions of HSF-1 target genes are in a more repressed state. This supports a model in which HSR genes are actively repressed, leading to reduced HSF-1 binding and diminished transcription in response to stress. Furthermore, our data suggest that a similar mechanism may dictate the repression of other cell stress response pathways in early adulthood.

The H3K27me3 demethylase *jmjd-3.1* controls the timing of stress response repression in adulthood

Levels of histone methylation are regulated by the interplay between specific methyltransferases and demethylases. In *C. elegans*, four conserved histone demethylases with activity against H3K27me3 are expressed, each of which has distinct expression patterns (Agger et al., 2007; Vandamme et al., 2012). To determine whether changes in the expression of H3K27me3 demethylases could account for increased H3K27me3 levels and HSR repression, we quantified the expression of these genes between day 1 and day 2 of adulthood. While the expression levels of *jmjd-3.2* were unchanged, the expression of two H3K27 demethylases, *utx-1* and *jmjd-3.1*, was altered at day 2 of adulthood (Figure 4D). The expression of *utx-1* increased by 30% and may constitute a lifespan relevant change early in adulthood (Jin et al., 2011; Maures et al., 2011). In contrast, the expression of *jmjd-3.1* declined by 60%, the timing of which precedes HSR decline (Figure 4D and E). Reduced *jmjd-3.1* expression is also observed in *gon-2* animals (Figure 4F), suggesting that a profound depletion of *jmjd-3.1* occurs in the soma. The expression of *jmjd-3.3* was increased in wild type but not *gon-2* animals suggesting that changes in *jmjd-3.3* expression do not occur in the adult soma (Figure 4D and Figure S4D). These data suggest that reduced *jmjd-3.1* levels could underlie the accumulation of H3K27me3 and transcriptional re-tuning at HS genes on the second day of adulthood.

To test the causal relationship between *jmjd-3.1* and the HSR, we took advantage of *jmjd-3.1* null mutants deficient in H3K27me3 demethylase activity and a well characterized *jmjd-3.1* transgenic line over-expressing a functional mCherry tagged *jmjd-3.1* under the control of endogenous promoter elements (Zuryn et al., 2014). *Jmjd-3.1* exhibits a diffuse nuclear pattern and is expressed in neurons as well as intestinal, muscle, and hypodermal cells at overall levels 30 fold higher than that of wild type worms (Figure S5A) (Vandamme et al., 2012; Zuryn et al., 2014). Consistent with a role for *jmjd-3.1* in the regulation of the HSR, *jmjd-3.1* mutant animals have increased H3K27me3 levels at HS loci (Figure 4G), exhibit a 60% reduction in stress induced expression of HS genes, have reduced survival at 35°C compared to wild type worms on day 1 of adulthood and recover poorly from a transient heat shock (Figures 5A-D). Furthermore, *jmjd-3.1* RNAi reduces thermorecovery of day 1 adults, whereas RNAi of other H3K27me3 demethylases has no effect (Figure S5B). Interestingly, HS gene induction and resistance to thermal stress are further decreased at day 2 of adulthood in *jmjd-3.1* mutants (Figures 5A, B and D) which could suggest that other factors also influence HSR collapse and stress resistance. Furthermore, the induction of

hsp-4, *gcs-1*, and *hsp-6* is also significantly reduced in stressed *jmjd-3.1* mutant animals on day 1 of adulthood (Figures 5E–G).

Consistent with the regulatory effects of *jmjd-3.1* on the HSR, over-expression of *jmjd-3.1* maintained the inducibility of stress response genes, increased thermotolerance and preserved the ability to recover from HS at day 2 of adulthood (Figures 5A–G, Table S1). In addition, over-expression of *jmjd-3.1* in day 2 adults increased median and maximal lifespan by $\approx 20\%$ and 12% respectively, suppressed age-related motility and pharyngeal pumping defects and decreased brood size by 20% (Figures 5H and S5C–E). These effects are independent of changes in the expression of *hsf-1* or other H3K27me3 demethylases (Figures S5F–H). Maintenance of stress resistance and increased lifespan were also observed in two independent integrated *jmjd-3.1* over-expression lines (Figure S5J and K). In contrast, over-expression of *jmjd-3.1* lacking a nuclear localization sequence ((this mutant does not enter the nucleus and therefore does not influence transcription (Zuryn et al., 2014)) failed to influence lifespan or stress resistance in early adulthood (Figure S5I–K). Thermotolerance was reduced in day 1 adult *jmjd-3.1* mutant animals; however, no difference in lifespan, motility or fecundity was observed (Figures 5H and S5C–E). Collectively, these results lead us to conclude that *jmjd-3.1* mediated control of H3K27me3 regulates multiple cell stress responses and stress resistance in early adulthood.

Signals from germ line stem cells re-tune the HSR through *jmjd-3.1* and H3K27me3 levels

HSR collapse coincides with the onset of reproduction, however, the absence of sperm, oocytes or the entire gonad has no effect on HSR decline (Figures S1G–J), suggesting that sterility alone cannot prevent repression of the HSR. The specific removal of germ line stem cells (GSCs) enhances proteostasis and increases lifespan, however, removal of the entire gonad does not have these effects, likely due to opposing signals from GSCs and the somatic gonad (Arantes-Oliveira et al., 2002; Shemesh et al., 2013). Therefore, we examined whether signals from the germ line are involved in the regulation of the HSR through *jmjd-3.1* and H3K27me3 levels. In contrast to the removal of oocytes, sperm or the entire gonad, reducing GSC number using two independent temperature sensitive mutants, *glp-1* and *glp-4*, that are defective in GSC proliferation (Wang et al., 2008), upholds the HSR, preserves *jmjd-3.1* expression and enhances stress resistance during adulthood (Figures 6A–C, S6A and S6B). Removal of GSCs also maintains transcription initiation at HS genes and completely suppresses the accumulation of H3K27me3 at HS loci on day 2 (Figures 6D, E and Figures S6C–H). These data suggest that reduced numbers of GSC preserves the HSR through maintenance of an optimal chromatin state. The fact that removal of the entire gonad (*gon-2* mutants) does not have these effects suggests that the effects of GSCs on the organism rely on an interplay with the somatic gonad as has been previously observed for the effects of GSCs on lifespan.

Removal of GSCs enhances stress resistance and extends lifespan through *jmjd-3.1*

To determine whether *jmjd-3.1* activity is necessary for suppression of H3K27me3 levels and maintenance of HS gene induction in response to removal of GSCs, we crossed *glp-1* mutants to *jmjd-3.1* null mutants. Consistent with effects observed in wild type animals (Figure 4G), *glp-1;jmjd-3.1* double mutants have increased levels of H3K27me3 at all stress

gene loci tested, suggesting that *jmjd-3.1* activity is necessary to suppress H3K27me3 at stress response genes (Figure 7A). *glp-1;jmjd-3.1* double mutants exhibited a 50% reduction in both HS gene induction following stress and in the ability to recover from an acute HS (Figures 7B and C). Furthermore, the enhanced thermotolerance and extended lifespan typically associated with *glp-1* mutants was significantly suppressed in *glp-1;jmjd-3.1* double mutants (Figures 7D and E). Similar effects were also observed through RNAi of *jmjd-3.1* but not with RNAi against other H3K27me3 demethylases (Figures S7A-E).

In summary, our data reveal the existence of a precise transcriptional switch that results in the repression of multiple cell stress response pathways as animals commit to reproduction. The re-tuning of stress responses occurs due to a shift towards a more repressed chromatin state, likely through increased H3K27me3 levels at stress gene loci, and the timing of this switch is controlled by the H3K27 demethylase *jmjd-3.1* in response to signals from GSCs. As such, we propose that the repression of cell stress response pathways is deployed at the organismal level to reset the proteostasis network in favor of reproduction over stress resistance, a model in keeping with the disposable soma theory of aging.

Discussion

Aging has long been thought to contribute to the onset of many degenerative diseases associated with protein misfolding as exemplified by neurodegenerative disorders. Yet, even for these pathologies it is uncertain whether an age-associated decline in protein quality control pathways represents a parallel or causative event. Here we show that multiple cell stress responses, highlighted by a dramatic collapse of the HSR, are severely compromised at an early point in adulthood that is associated with fecundity. This repression of cell stress responses has profound consequences on stress resilience during adulthood and organismal lifespan, and may leave adults more vulnerable to disease.

Our results show that the HSR of *C. elegans* is repressed within a four hour window that is coincident with the onset of egg-laying on the first day of adulthood. The physical act of laying eggs is unlikely to signal this event as mutants devoid of sperm or eggs still undergo dramatic re-tuning of the HSR. Instead, we propose that the timing of stress response collapse is controlled by the H3K27 demethylase *jmjd-3.1* in response to signals from GSCs (Figure 7F). GSC number expands during larval development and continues to increase after the onset of egg-laying suggesting that neither initiation nor cessation of GSC proliferation dictates repression of the HSR. Instead it would appear that the stress response switch is coordinated to occur as animals commit to egg-laying, possibly due to a series of environmental cues that are sensed by the germ line. Our data suggest that stress response pathways are not gradually and progressively dysregulated as a consequence of stochastic damage with age but are instead rapidly and precisely repressed as animals commit to reproduction. While we have not categorically ruled out the possibility that early changes in the protein folding environment contribute to repression of stress responses, our data suggest that the transition to reproductive maturity represents a period of significant change for the PN and the proteome and support a model whereby commitment to optimal fecundity occurs at the expense of somatic stress resistance. We suggest that this logic may be important for free-living organisms to ensure that adult animals do not compete for limiting resources.

Prioritization of resources to the germ line to maximize reproduction is consistent with the disposable soma theory of aging (Kirkwood, 1977). In addition, dampening stress responses may provide sufficient protection for animals to complete reproduction whilst gradually accumulating damage. This could expedite parental death to save space and resources for future generations.

The revelation that *jmjd-3.1* activity and levels of H3K27me3 at stress response gene loci dictate the timing of HSR collapse in response to signals from GSCs makes a compelling argument that a coordinated genetic process contributes to organismal susceptibility to disease. H3K27me3 however, is primarily associated with development and differentiation (Voigt et al., 2013), therefore it is perhaps surprising that our data support a central role for *jmjd-3.1* and H3K27me3 in the maintenance of somatic health and stress resistance during *C. elegans* adulthood. *D. melanogaster E(z)* and *Esc* mutants exhibit increased H3K27me3 levels, shortened lifespans and reduced tolerance to thermal stress in adulthood, suggesting that increased H3K27me3 levels can have detrimental effects on organismal health (Siebold et al., 2010). However, previous studies in *C. elegans* suggest that maintaining H3K27me3 levels through reduced activity of the H3K27 demethylase *utx-1* is beneficial, resulting in lifespan extension and increased stress resistance (Jin et al., 2011; Maures et al., 2011). We suggest that *utx-1* and *jmjd-3.1* have opposing roles in the maintenance of somatic health and that increased H3K27me3 levels can be beneficial or detrimental depending on the genomic loci modified. Recent studies of the human orthologs of *utx-1* and *jmjd-3.1* have shown that despite similar enzymatic activity, H3K27 demethylases control distinct transcriptional programs in T-cell acute lymphoblastic leukaemia (Ntziachristos et al., 2014), therefore, it is possible that a similar system is in place in *C. elegans* to control gene expression in adulthood. Furthermore, it is also likely that *utx-1* and *jmjd-3.1* have different spatial and temporal patterns of activity which result in differential effects on aging and stress resistance (Vandamme et al., 2012).

Organisms must integrate physiological and environmental signals with the activity of the PN and stress response pathways. This has led to the evolution of cell non-autonomous control of the PN through neuronal signaling and transcellular chaperone signaling (Prahlad et al., 2008; van Oosten-Hawle et al., 2013). GSCs also exert cell non-autonomous effects on somatic proteostasis (Lapierre et al., 2011; Shemesh et al., 2013; Vilchez et al., 2012), however, it was unknown how signals from the germ line influence the PN. Our data provide evidence that GSCs can regulate somatic cell stress responses by controlling the chromatin state at stress gene loci. This could explain the widespread effects of GSC removal on the PN and it will therefore be important to determine the genomic targets of *jmjd-3.1*. Our data suggest that the HSR, and perhaps all stress responses in the soma, are dependent upon the reproductive potential of the entire animal.

In summary, we have identified a cell stress response switch that marks the onset of reproduction in *C. elegans* and is controlled by changes in H3K27 methylation. As such, we propose that collapse of the HSR and other cell stress responses is a key feature of a program to maximize reproduction at the expense of stress resistance, and may be among the earliest events governing healthy aging in metazoans. Our findings support a view that long-

term health is set before the cessation of reproduction, and that early life changes modulated by signals from the germ line trigger proteostasis collapse, cellular dysfunction and aging.

Experimental procedures

Worm maintenance conditions

C. elegans strains were maintained and handled using standard techniques (Brenner, 1974). All experiments were performed at 20°C unless stated. Worms were age-synchronized by egg-laying with the exception of worms used for ChIP, DNase and EMSA assays which were age-synchronized by bleaching. Mutant *C. elegans* strains were obtained from the *Caenorhabditis* genetics center (CGC) and were backcrossed at least 5 times before use. RNAi was performed by feeding as previously described (Kamath et al., 2003). Transgenic worms over-expressing *jmjd-3.1::mCherry* (AM1107) as an extrachromosomal array were generated by back crossing strain IS1427 (*jmjd-3.1(fp15); syls63 [cog-1p::GFP ; unc-119(+)] ; fpEx355 [jmjd-3.1p::jmjd-3.1::mCherry, odr-1::dsRed]*) (Zuryn et al., 2014) to Bristol N2 worms seven times to remove the *fp15* mutation and the *syIs63* transgene. Animals containing the *jmjd-3.1p::jmjd-3.1::mCherry* transgene were selected by following the *odr-1::RFP* co-injection marker. Integrated lines expressing wild type *jmjd-3.1::mCherry* (lines AM1110 and AM1111) or *jmjd-3.1delNLS::mCherry* (lines AM1112 and AM1114) were generated by exposing lines expressing extrachromosomal arrays of the indicated transgenes along with the co-injection marker to gamma irradiation from caesium¹³⁷ for 18 minutes. Strains expressing extrachromosomal arrays of *jmjd-3.1delNLS::mCherry* were derived by back crossing strain IS1572 (*jmjd-3.1 (fp15); syls63 [cog-1p::GFP ; unc-119(+)] ; fpEx422 [jmjd-3.1p::jmjd-3.1delNLS::mCherry, myo-2::mCherry]*) to N2 worms to remove the *fp15* mutation and the *syIs63* transgene. Positive integrants were detected by genotyping worms expressing the co-injection marker. Animals were backcrossed at least 7 times to wild type N2 animals before use. For a complete list of worm strains used please see supplemental materials.

Scoring brood size

Age synchronized animals were singled on OP50 seeded NGM plates and allowed to lay eggs for a period of 24 hours. Worms were then transferred to new plates and eggs were allowed to hatch and grow to L3 stage at which point the number of progeny was counted by removing and flaming all worms.

Monitoring the timing of egg-laying

C. elegans were maintained at indicated temperatures until the L4/YA stage. Upon exit from L4, worms were singled onto OP50 seeded NGM plates and scored every 2 hours for the number of eggs laid (as detected by eye using a Leica light microscope). A parallel set of plates were also monitored for the gross appearance of eggs to ensure that the timing of egg-laying was not affected by the singling of worms.

Scoring age-related decline in pharyngeal pumping

The number of pharyngeal contractions per minute was scored by monitoring individual worms on plates and counting the number of contractions every 10 seconds. This was

performed at least 5 times for each worm and the average number of contractions per 10 seconds was used to calculate contractions per minute per worm.

Scoring age-related decline in motility

Motility defects were measured through life by assessing the ability of animals to move in response to plate tapping. Worms were scored as having motility defects when unresponsive to plate tap due to paralysis or when displaying uncoordinated movement.

Heat shock conditions

Heat shock was performed on solid NGM plates in a water bath pre-heated to 33°C (unless stated otherwise). Plates were wrapped with parafilm and submerged for 30 minutes. Animals were harvested immediately following heat shock and snap frozen in liquid nitrogen.

Treatment with DTT, tunicamycin, paraquat and ethidium bromide

Worms were exposed to chemical stress by incubation in M9 supplemented with paraquat (200 mM), DTT (3 mM), tunicamycin (100 µg/ml) or ethidium bromide (800 µg/ml) for 2, 7, 3 or 8 hours respectively. Worms were harvested, washed 3 times with M9 and snap frozen in liquid nitrogen.

Stress resistance assays

Thermotolerance and DTT resistance were measured on OP50 seeded NGM plates maintained at 35°C or supplemented with 10 mM DTT respectively. Survival was scored every 2 (thermotolerance) or 24 (DTT) hours by absence of touch response or pharyngeal pumping. Paraquat resistance was assayed by immersing worms in M9 supplemented with OP50 and 200 mM paraquat in 12 well polypropylene plates. Survival was determined by absence of touch response.

Thermorecovery

To assess the ability of *C. elegans* to recover from thermal stress, worms were heat shocked at 33°C for 6 hours on NGM plates and then returned to standard maintenance conditions for 48 hours. Worms were scored for their ability to crawl onto OP50 seeded NGM plates and were classified as moving normally when able to immediately crawl away with no signs of abnormal, jerky movement or paralysis. No more than 40 worms were present on each plate. Thermorecovery was measured after a 34°C HS in animals raised at 25°C.

Lifespan assays

Age-synchronized worms were scored as dead and removed in the absence of touch response or pharyngeal pumping. Worms were transferred to fresh plates everyday from day 1 to day 5 of adulthood to remove progeny and transferred every other day from then on. Bagged, desiccated or missing animals were censored from analysis.

Real time quantitative PCR

RNA was extracted using Trizol and Qiagen RNeasy RNA extraction columns as per manufacturers' instructions. cDNA synthesis was performed using iScript reverse transcription mix (BioRad) and real time quantitative PCR was performed using SYBR green PCR reaction mixture (BioRad) in a BioRad iCycler iQ real time PCR detection system with the following conditions: (15s at 95°C, 20s at 56°C, 30s at 72°C) × 39 cycles. Relative expression was calculated from Cycle threshold values using the standard curve method and the expression of genes of interest was normalized to the housekeeping genes *cdc-42* and *rpb-2*.

Electrophoretic mobility shift assays

EMSA assays were essentially performed as previously described (van Oosten-Hawle et al., 2013) with slight modifications. Binding reactions contained 40 µg of nuclear protein, 1 ng of oligonucleotide probe, 10 µg of BSA and 2 µg of poly(dI.dC). Binding reactions were allowed to proceed for 30 min at room temperature before samples were separated on a 4% native polyacrylamide gel. Phosphorescence was imaged using a STORM-860 phosphor-imager. The relative intensity of HSF-1::HSE bands was quantified using image J. For clarity, images were cropped and brightness/contrast was adjusted across the entire image using Adobe Photoshop.

Fluorescence microscopy

Worms were imaged by mounting on 5% agarose pads in 3 mM levamisole. Images of reporter worms were acquired using a Zeiss Axiovert 200 microscope, a Hamamatsu Orca 100 cooled CCD camera and Zeiss axiovision software. Images of HSF-1::GFP were captured using a Leica SP5 II laser scanning confocal microscope equipped with a 100X/1.4 N.A. oil immersion lens and HyD detectors. Acquisition parameters were kept identical across samples. For clarity, images were cropped and brightness/contrast was adjusted across the entire image using Adobe Photoshop.

Chromatin immunoprecipitation

ChIP was essentially performed as previously described (Mukhopadhyay et al., 2008) with slight modifications. Worms were cross-linked with 2% formaldehyde, washed and re-suspended in lysis buffer. Worms were lysed and sonicated to yield 500bp – 1kb size DNA fragments. Pull downs were performed using 2µg chromatin, protein g-dynabeads and 2 µg of antibody at 4°C with rotation over night. Following washing and elution DNA was recovered using Qiagen PCR purification kit as per manufacturer's instructions. Strain OG497 was used for HSF-1 ChIP to minimize signal from the germ line (Morton and Lamitina, 2013; Tatum et al., 2015). A complete list of primers and antibodies used in these experiments can be found in supplementary tables 1 and 2. Please see supplemental materials for more detailed information.

DNase I digestion assay

DNase I digestion assays were essentially performed as previously described with slight modifications (Dorschner et al., 2004). The relative degree of digestion at genomic regions

in chromatin from day 2 animals relative to day 1 adults was calculated and plotted in order to provide a less counter-intuitive view of the data. Please see supplemental materials for more detailed information.

Protein extraction and western blotting

Standard methods for western blotting were used for the detection of HSP-16 and tubulin. Briefly, 5 µg of *C. elegans* protein lysate in Laemmli loading buffer was separated by SDS-PAGE and transferred to nitrocellulose membranes. Anti HSP-16 (1:1000; overnight at 4°C) or anti-tubulin primary antibodies (1:5000; 1 hour at room temperature) and HRP conjugated secondary antibodies (1:5000; 1 hour at room temperature) were used to probe blots. Please see supplemental materials for additional information.

Statistical analyses

Statistical significance was calculated by unpaired, two-tailed Student's *t*-test in Microsoft excel or one or two-way ANOVA with Tukey or Bonferroni post analysis pair wise comparison in GraphPad Prism. Lifespan statistics were calculated by Log-rank (Mantel-Cox) test using OASIS online lifespan analysis software <http://sbi.postech.ac.kr/oasis>.

Supplementary Material

Refer to Web version on PubMed Central for supplementary material.

Acknowledgements

These studies were supported by a Postdoctoral Fellowship to J.L. from the ALS Association and grants from the National Institutes of Health (NIGMS, NIA, NIMH), the Ellison Medical Foundation, and the Daniel F. and Ada L. Rice Foundation to R.I.M. The authors thank the members of the Morimoto Laboratory for their support and critical reading of the manuscript. We also thank Steven Zury and Sophie Jarrault for *jmjd-3.1* over-expression line IS1427 and IS1572, the Lithgow lab (Buck institute) for anti HSP-16.2 antibody and the Northwestern university Biological Imaging Facility and Keck biophysics facilities for instrument use.

References

- Agger K, Cloos PA, Christensen J, Pasini D, Rose S, Rappsilber J, Issaeva I, Canaani E, Salcini AE, Helin K. UTX and JMJD3 are histone H3K27 demethylases involved in HOX gene regulation and development. *Nature*. 2007; 449:731–734. [PubMed: 17713478]
- Akerfelt M, Morimoto RI, Sistonen L. Heat shock factors: integrators of cell stress, development and lifespan. *Nature reviews Molecular cell biology*. 2010; 11:545–555. [PubMed: 20628411]
- Arantes-Oliveira N, Apfeld J, Dillin A, Kenyon C. Regulation of life-span by germ-line stem cells in *Caenorhabditis elegans*. *Science*. 2002; 295:502–505. [PubMed: 11799246]
- Ben-Zvi A, Miller EA, Morimoto RI. Collapse of proteostasis represents an early molecular event in *Caenorhabditis elegans* aging. *Proceedings of the National Academy of Sciences of the United States of America*. 2009; 106:14914–14919. [PubMed: 19706382]
- Brenner S. The genetics of *Caenorhabditis elegans*. *Genetics*. 1974; 77:71–94. [PubMed: 4366476]
- David DC, Ollikainen N, Trinidad JC, Cary MP, Burlingame AL, Kenyon C. Widespread protein aggregation as an inherent part of aging in *C. elegans*. *PLoS biology*. 2010; 8:e1000450. [PubMed: 20711477]
- Dorschner MO, Hawrylycz M, Humbert R, Wallace JC, Shafer A, Kawamoto J, Mack J, Hall R, Goldy J, Sabo PJ, et al. High-throughput localization of functional elements by quantitative chromatin profiling. *Nature methods*. 2004; 1:219–225. [PubMed: 15782197]

- Egelhofer TA, Minoda A, Klugman S, Lee K, Kolasinska-Zwierz P, Alekseyenko AA, Cheung MS, Day DS, Gadel S, Gorchakov AA, et al. An assessment of histone-modification antibody quality. *Nature structural & molecular biology*. 2011; 18:91–93.
- Haynes CM, Fiorese CJ, Lin YF. Evaluating and responding to mitochondrial dysfunction: the mitochondrial unfolded-protein response and beyond. *Trends in cell biology*. 2013; 23:311–318. [PubMed: 23489877]
- Henis-Korenblit S, Zhang P, Hansen M, McCormick M, Lee SJ, Cary M, Kenyon C. Insulin/IGF-1 signaling mutants reprogram ER stress response regulators to promote longevity. *Proceedings of the National Academy of Sciences of the United States of America*. 2010; 107:9730–9735. [PubMed: 20460307]
- Hirsh D, Oppenheim D, Klass M. Development of the reproductive system of *Caenorhabditis elegans*. *Developmental biology*. 1976; 49:200–219. [PubMed: 943344]
- Hoogewijs D, Houthoofd K, Matthijssens F, Vandesompele J, Vanfleteren JR. Selection and validation of a set of reliable reference genes for quantitative sod gene expression analysis in *C. elegans*. *BMC molecular biology*. 2008; 9:9. [PubMed: 18211699]
- Hsu AL, Murphy CT, Kenyon C. Regulation of aging and age-related disease by DAF-16 and heat-shock factor. *Science*. 2003; 300:1142–1145. [PubMed: 12750521]
- Huang S, Ling JJ, Yang S, Li XJ, Li S. Neuronal expression of TATA box-binding protein containing expanded polyglutamine in knock-in mice reduces chaperone protein response by impairing the function of nuclear factor-Y transcription factor. *Brain : a journal of neurology*. 2011; 134:1943–1958. [PubMed: 21705419]
- Jin C, Li J, Green CD, Yu X, Tang X, Han D, Xian B, Wang D, Huang X, Cao X, et al. Histone demethylase UTX-1 regulates *C. elegans* life span by targeting the insulin/IGF-1 signaling pathway. *Cell metabolism*. 2011; 14:161–172. [PubMed: 21803287]
- Kamath RS, Fraser AG, Dong Y, Poulin G, Durbin R, Gotta M, Kanapin A, Le Bot N, Moreno S, Sohrmann M, et al. Systematic functional analysis of the *Caenorhabditis elegans* genome using RNAi. *Nature*. 2003; 421:231–237. [PubMed: 12529635]
- Kirkwood TB. Evolution of ageing. *Nature*. 1977; 270:301–304. [PubMed: 593350]
- Labbadia J, Cunliffe H, Weiss A, Katsyuba E, Sathasivam K, Seredenina T, Woodman B, Moussaoui S, Frentzel S, Luthi-Carter R, et al. Altered chromatin architecture underlies progressive impairment of the heat shock response in mouse models of Huntington disease. *The Journal of clinical investigation*. 2011; 121:3306–3319. [PubMed: 21785217]
- Labbadia J, Morimoto RI. The Biology of Proteostasis in Aging and Disease. *Annual review of biochemistry*. 2015; 84:435–464.
- Lapierre LR, Gelino S, Melendez A, Hansen M. Autophagy and lipid metabolism coordinately modulate life span in germline-less *C. elegans*. *Current biology : CB*. 2011; 21:1507–1514. [PubMed: 21906946]
- Maures TJ, Greer EL, Hauswirth AG, Brunet A. The H3K27 demethylase UTX-1 regulates *C. elegans* lifespan in a germline-independent, insulin-dependent manner. *Aging cell*. 2011; 10:980–990. [PubMed: 21834846]
- Morimoto RI. Proteotoxic stress and inducible chaperone networks in neurodegenerative disease and aging. *Genes & development*. 2008; 22:1427–1438. [PubMed: 18519635]
- Morley JF, Morimoto RI. Regulation of longevity in *Caenorhabditis elegans* by heat shock factor and molecular chaperones. *Molecular biology of the cell*. 2004; 15:657–664. [PubMed: 14668486]
- Morton EA, Lamitina T. *Caenorhabditis elegans* HSF-1 is an essential nuclear protein that forms stress granule-like structures following heat shock. *Aging cell*. 2013; 12:112–120. [PubMed: 23107491]
- Mukhopadhyay A, Deplancke B, Walhout AJ, Tissenbaum HA. Chromatin immunoprecipitation (ChIP) coupled to detection by quantitative real-time PCR to study transcription factor binding to DNA in *Caenorhabditis elegans*. *Nature protocols*. 2008; 3:698–709. [PubMed: 18388953]
- Ntziachristos P, Tsirigos A, Welstead GG, Trimarchi T, Bakogianni S, Xu L, Loizou E, Holmfeldt L, Strikoudis A, King B, et al. Contrasting roles of histone 3 lysine 27 demethylases in acute lymphoblastic leukaemia. *Nature*. 2014; 514:513–517. [PubMed: 25132549]

- Olzscha H, Schermann SM, Woerner AC, Pinkert S, Hecht MH, Tartaglia GG, Vendruscolo M, Hayer-Hartl M, Hartl FU, Vabulas RM. Amyloid-like aggregates sequester numerous metastable proteins with essential cellular functions. *Cell*. 2011; 144:67–78. [PubMed: 21215370]
- Prahlad V, Cornelius T, Morimoto RI. Regulation of the cellular heat shock response in *Caenorhabditis elegans* by thermosensory neurons. *Science*. 2008; 320:811–814. [PubMed: 18467592]
- Rea SL, Wu D, Cypser JR, Vaupel JW, Johnson TE. A stress-sensitive reporter predicts longevity in isogenic populations of *Caenorhabditis elegans*. *Nature genetics*. 2005; 37:894–898. [PubMed: 16041374]
- Reis-Rodrigues P, Czerwieniec G, Peters TW, Evani US, Alavez S, Gaman EA, Vantipalli M, Mooney SD, Gibson BW, Lithgow GJ, et al. Proteomic analysis of age-dependent changes in protein solubility identifies genes that modulate lifespan. *Aging cell*. 2012; 11:120–127. [PubMed: 22103665]
- Shemesh N, Shai N, Ben-Zvi A. Germline stem cell arrest inhibits the collapse of somatic proteostasis early in *Caenorhabditis elegans* adulthood. *Aging cell*. 2013; 12:814–822. [PubMed: 23734734]
- Shore DE, Carr CE, Ruvkun G. Induction of cytoprotective pathways is central to the extension of lifespan conferred by multiple longevity pathways. *PLoS genetics*. 2012; 8:e1002792. [PubMed: 22829775]
- Siebold AP, Banerjee R, Tie F, Kiss DL, Moskowitz J, Harte PJ. Polycomb Repressive Complex 2 and Trithorax modulate *Drosophila* longevity and stress resistance. *Proceedings of the National Academy of Sciences of the United States of America*. 2010; 107:169–174. [PubMed: 20018689]
- Syktotis GP, Bohmann D. Stress-activated cap'n'collar transcription factors in aging and human disease. *Science signaling*. 2010; 3:re3. [PubMed: 20215646]
- Tatum MC, Ooi FK, Chikka MR, Chauve L, Martinez-Velazquez LA, Steinbusch HW, Morimoto RI, Prahlad V. Neuronal serotonin release triggers the heat shock response in *C. elegans* in the absence of temperature increase. *Current biology : CB*. 2015; 25:163–174. [PubMed: 25557666]
- Taylor RC, Dillin A. XBP-1 is a cell-nonautonomous regulator of stress resistance and longevity. *Cell*. 2013; 153:1435–1447. [PubMed: 23791175]
- Tullet JM, Hertweck M, An JH, Baker J, Hwang JY, Liu S, Oliveira RP, Baumeister R, Blackwell TK. Direct inhibition of the longevity-promoting factor SKN-1 by insulin-like signaling in *C. elegans*. *Cell*. 2008; 132:1025–1038. [PubMed: 18358814]
- van Oosten-Hawle P, Porter RS, Morimoto RI. Regulation of organismal proteostasis by transcellular chaperone signaling. *Cell*. 2013; 153:1366–1378. [PubMed: 23746847]
- Vandamme J, Lettier G, Sidoli S, Di Schiavi E, Norregaard Jensen O, Salcini AE. The *C. elegans* H3K27 demethylase UTX-1 is essential for normal development, independent of its enzymatic activity. *PLoS genetics*. 2012; 8:e1002647. [PubMed: 22570628]
- Vilchez D, Morante I, Liu Z, Douglas PM, Merkwirth C, Rodrigues AP, Manning G, Dillin A. RPN-6 determines *C. elegans* longevity under proteotoxic stress conditions. *Nature*. 2012; 489:263–268. [PubMed: 22922647]
- Voigt P, Tee WW, Reinberg D. A double take on bivalent promoters. *Genes & development*. 2013; 27:1318–1338. [PubMed: 23788621]
- Walter P, Ron D. The unfolded protein response: from stress pathway to homeostatic regulation. *Science*. 2011; 334:1081–1086. [PubMed: 22116877]
- Wang MC, O'Rourke EJ, Ruvkun G. Fat metabolism links germline stem cells and longevity in *C. elegans*. *Science*. 2008; 322:957–960. [PubMed: 18988854]
- Zuryn S, Ahier A, Portoso M, White ER, Morin MC, Margueron R, Jarriault S. Transdifferentiation. Sequential histone-modifying activities determine the robustness of transdifferentiation. *Science*. 2014; 345:826–829. [PubMed: 25124442]

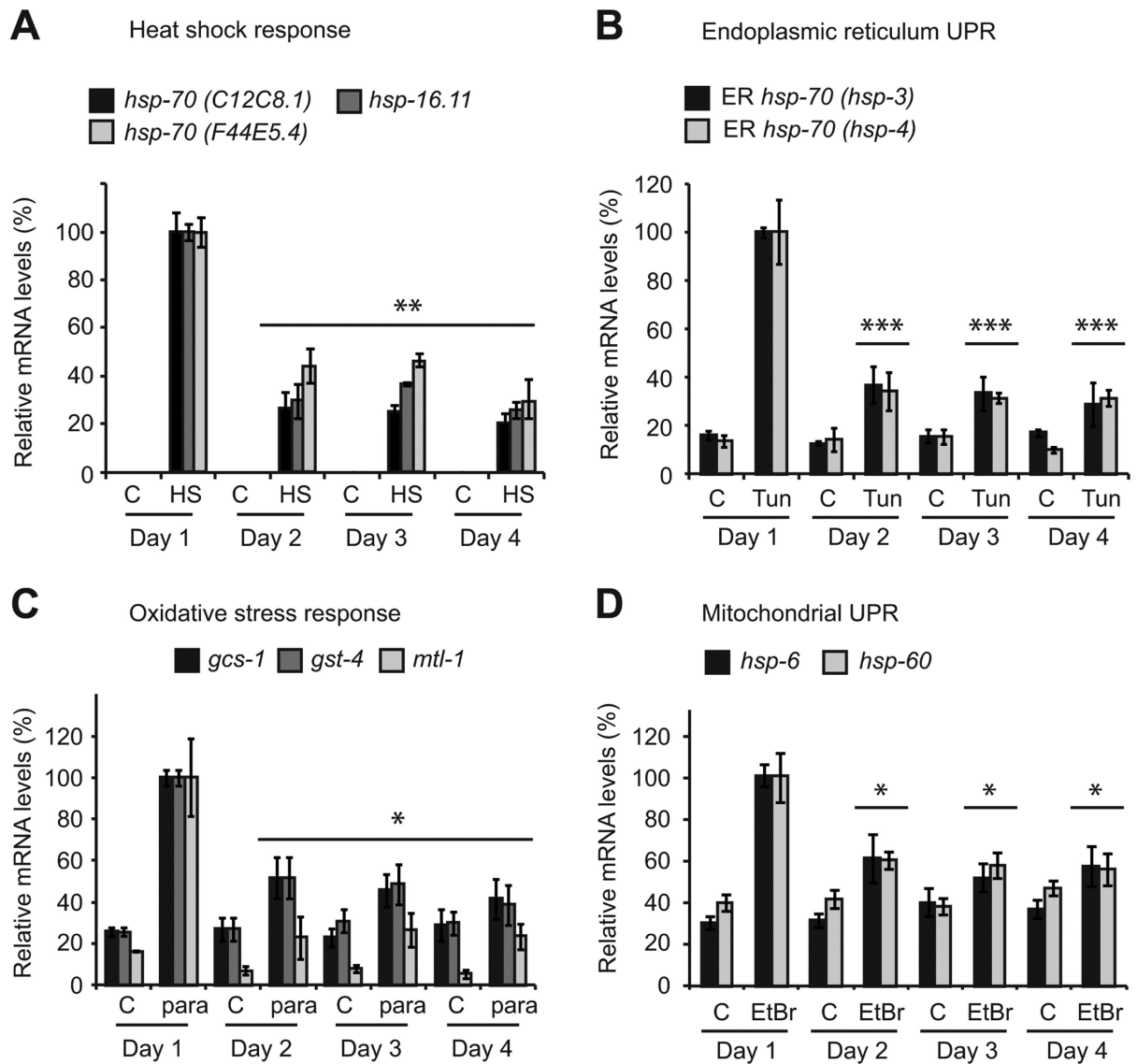


Figure 1. Multiple stress responses collapse within the first 24 hours of adulthood

Stress gene expression relative to *rpb-2* and *cdc-42* in adult animals maintained at 15°C and subjected to control (c) conditions or (A) heat shock (HS) at 33°C for 30 min, (B) 100 µg/ml tunicamycin (Tun) for 3 hours (C) 200 mM paraquat (para) for 2 hours or (D) 800 µg/ml Ethidium Bromide (EtBr) for 8 hours. Values plotted are the mean of 4 experimental replicates and error bars denote SEM. Statistical significance was calculated using one-way ANOVA with Tukey post analysis comparison of groups. * $p < 0.05$, ** $p < 0.01$, *** $p < 0.001$. Statistical comparisons denote the largest p -value within each treatment group for each gene relative to day 1 treatment. See also figure S1.

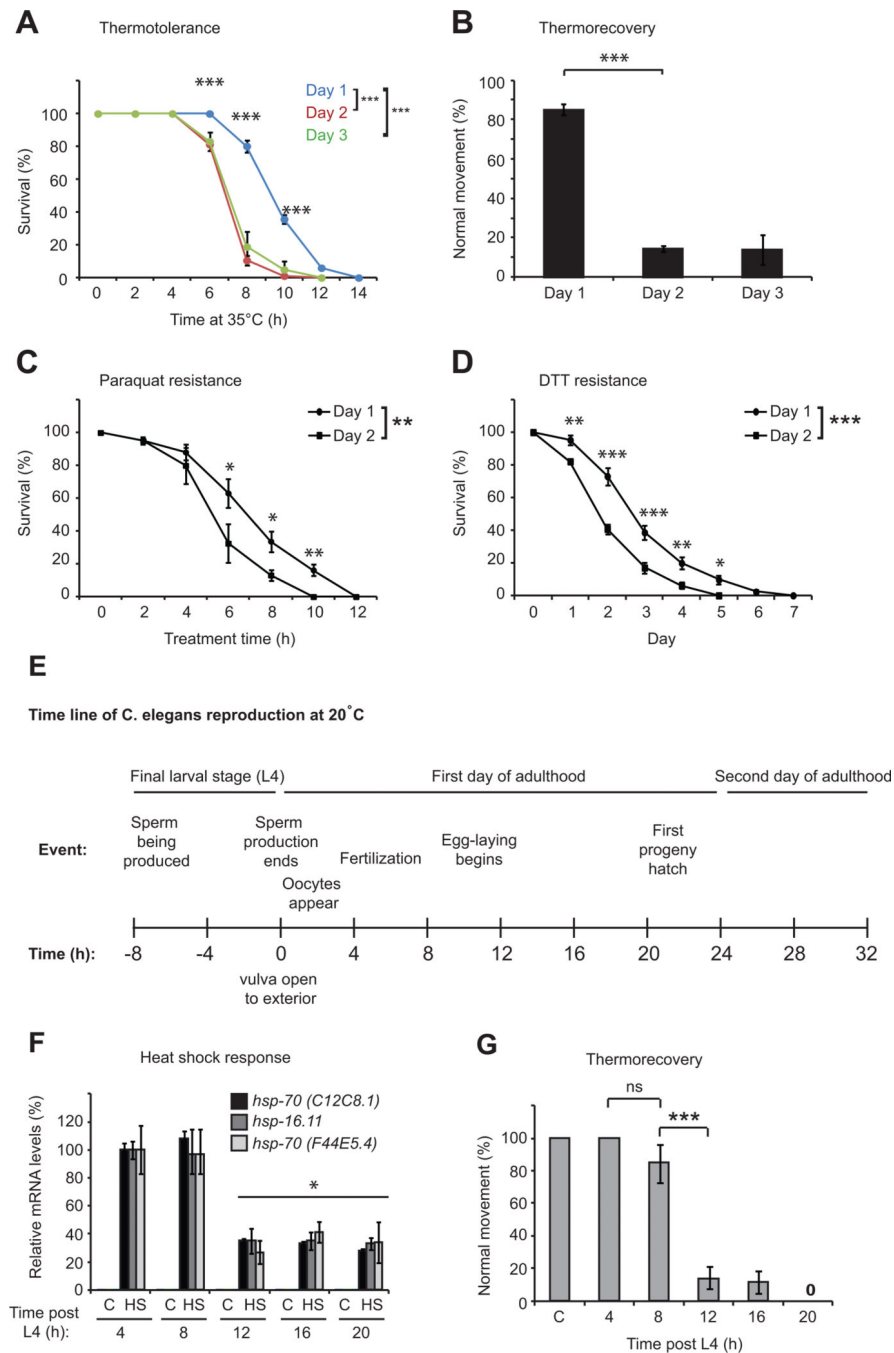


Figure 2. The heat shock response and stress resistance decline within a 4 hour window at the onset of egg-laying

(A) Survival of animals at 35°C. (B) Thermorecovery of worms exposed to 33°C heat shock for 6 hours and allowed to recover at 20°C for 48 hours. (C and D) Survival of *C. elegans* exposed to (C) 200 mM paraquat or (D) 10 mM DTT as day 1 or 2 adults. (E) Schematic of prominent reproductive events spanning the transition from the end of the final larval (L4) stage to peak egg-laying. Time in hours should be multiplied by 1.5 or 0.7 to obtain approximate timing of events at 15°C and 25°C respectively (Hirsh et al., 1976). Values plotted in each panel are the mean of at least 4 experimental replicates. Error bars represent

SEM. Statistical significance was calculated using one-way ANOVA with Tukey post analysis comparison of groups (B, F and G) or two-way ANOVA with Bonferroni post analysis comparison (A, C and D). * $p < 0.05$, ** $p < 0.01$, *** $p < 0.001$, not significant (ns) $p > 0.05$. See also figure S2.

Author Manuscript

Author Manuscript

Author Manuscript

Author Manuscript

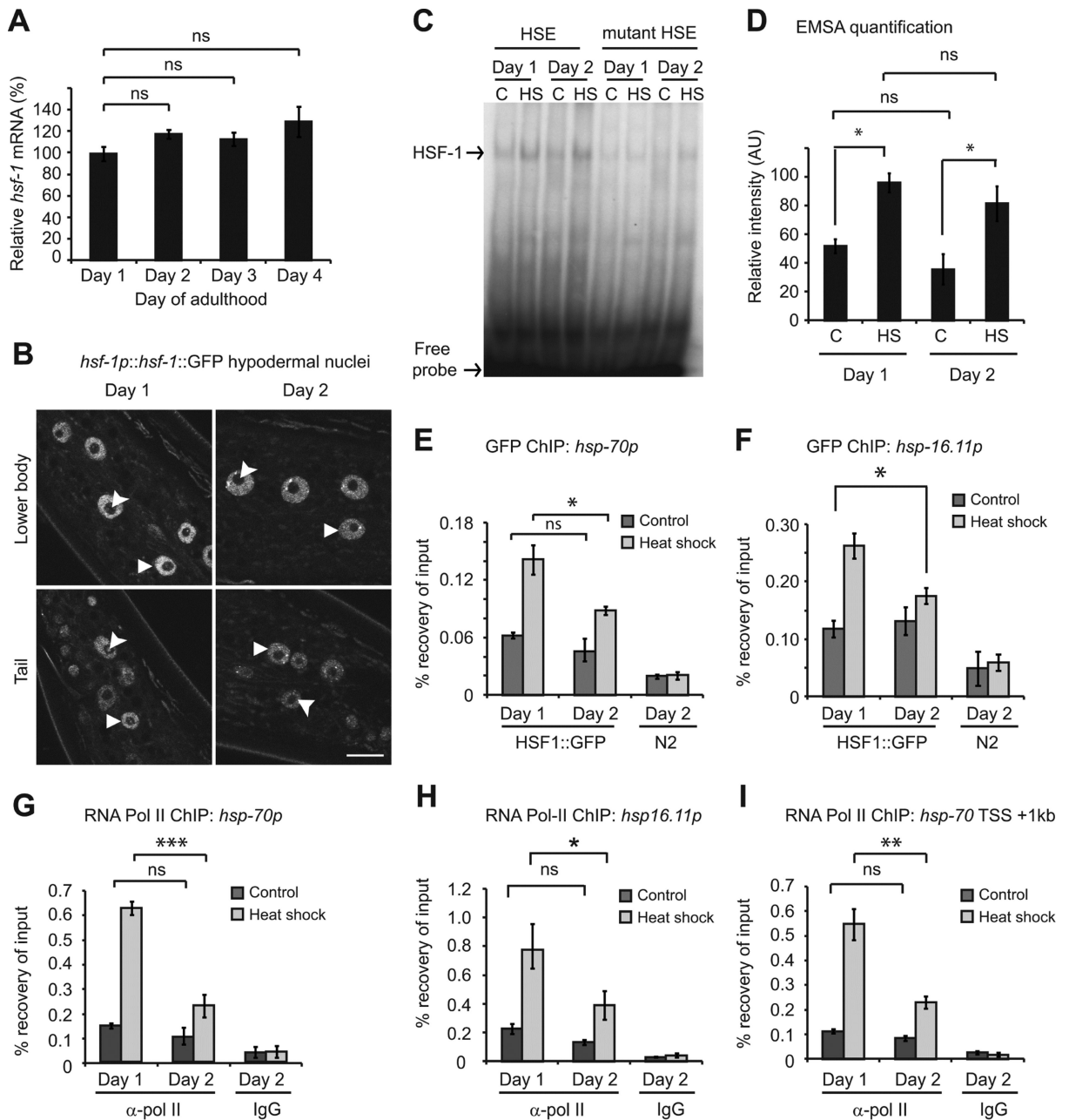


Figure 3. Altered chromatin landscape underlies collapse of the heat shock response

(A) *hsf-1* expression relative to *rpb-2* and *cdc-42*. (B) Confocal microscopy of HSF-1::GFP nuclear localization in hypodermal cells of day 1 (L4 + 4 hours) and day 2 (L4 + 28 hours) adults. Triangles and arrow heads highlight the nucleus and nucleolus respectively of select hypodermal cells. Scale bar = 10 μ m. (C) HSF-1 gel shift assay using DNA Probes containing intact or mutant versions of the HSF-1 consensus binding motif (HSE). (D) Quantification of HSF-1 gel shift experiments. ChIP-qPCR on HSF-1::GFP worms using (E and F) anti-GFP or (G - I) anti RNA pol-II (*ama-1*) antibodies. For a schematic of the regions amplified see Fig.S3D. Values plotted are the mean of at least 4 biological replicates except in the case of panel D where means are from 3 independent experiments. Error bars

represent SEM. Statistical significance was calculated by one-way ANOVA with Tukey post analysis comparison (A) or two-way ANOVA with Bonferroni post analysis comparison (D-I). * $p < 0.05$, ** $p < 0.01$, *** $p < 0.001$, not significant (ns) $p > 0.05$. See also figure S3.

Author Manuscript

Author Manuscript

Author Manuscript

Author Manuscript

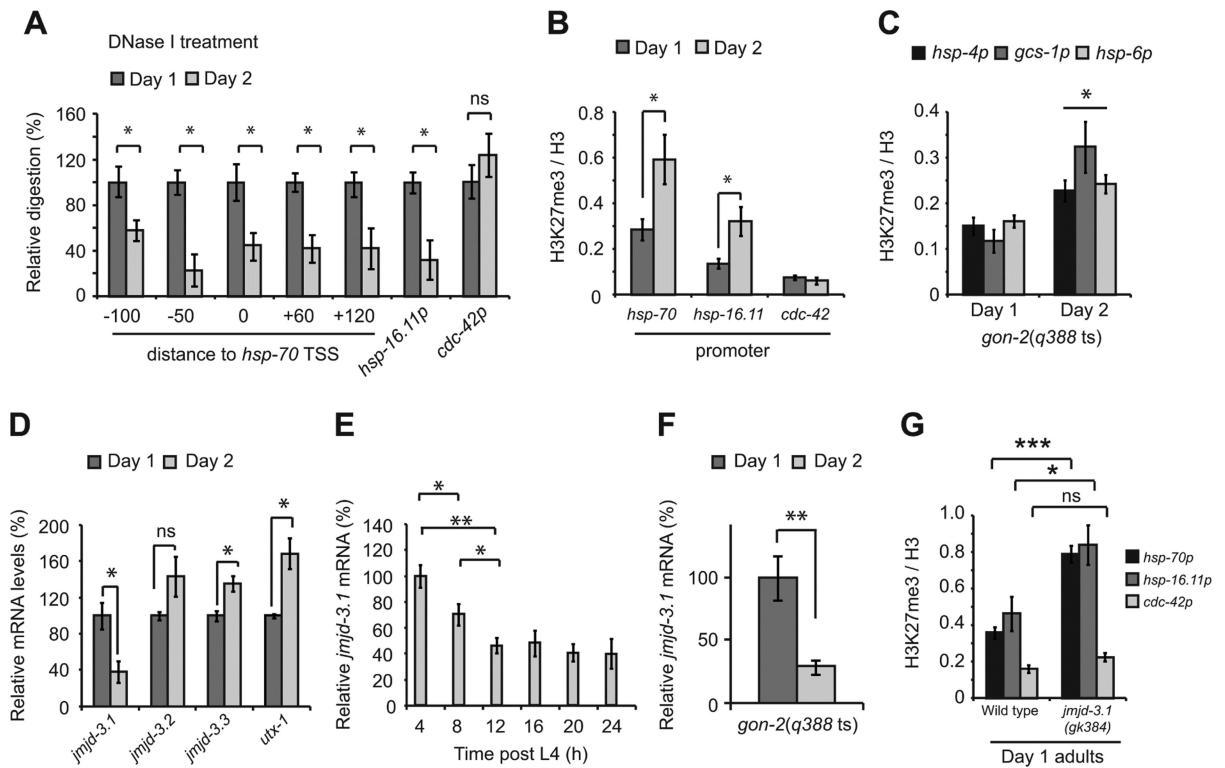


Figure 4. Increased H3K27me3 and repression of heat shock gene induction is due to reduced *jmjd-3.1* expression

(A) DNase I digestion of chromatin isolated from *gon-2(q388ts)* animals. Values are plotted as the relative degree of digestion compared to day 1 adults for each genomic region. (B and C) H3K27me3 ChIP-qPCR on *gon-2(q388ts)* worms. (D–F) H3K27me3 demethylase expression relative to *rpb-2* in (D and E) wild type (WT) or (F) *gon-2(q388ts)* worms. (G) H3K27me3 ChIP-qPCR in WT and *jmjd-3.1(gk384)* null mutants. Primers used were the same as those in HSF-1 and RNA pol-2 ChIP-qPCR experiments. Values plotted in panel A are the mean of at least 3 biological replicates. All other values plotted are the mean of at least 4 biological replicates and error bars represent SEM. Statistical significance was calculated by Student's *t*-test (A–D, F and G) or one-way ANOVA with Tukey post analysis comparison (E) * $p < 0.05$, ** $p < 0.01$, *** $p < 0.001$, ns $p > 0.05$. TSS = Transcription start site. *hsp-70p* = promoter of *C12C8.1*. See also figure S4.

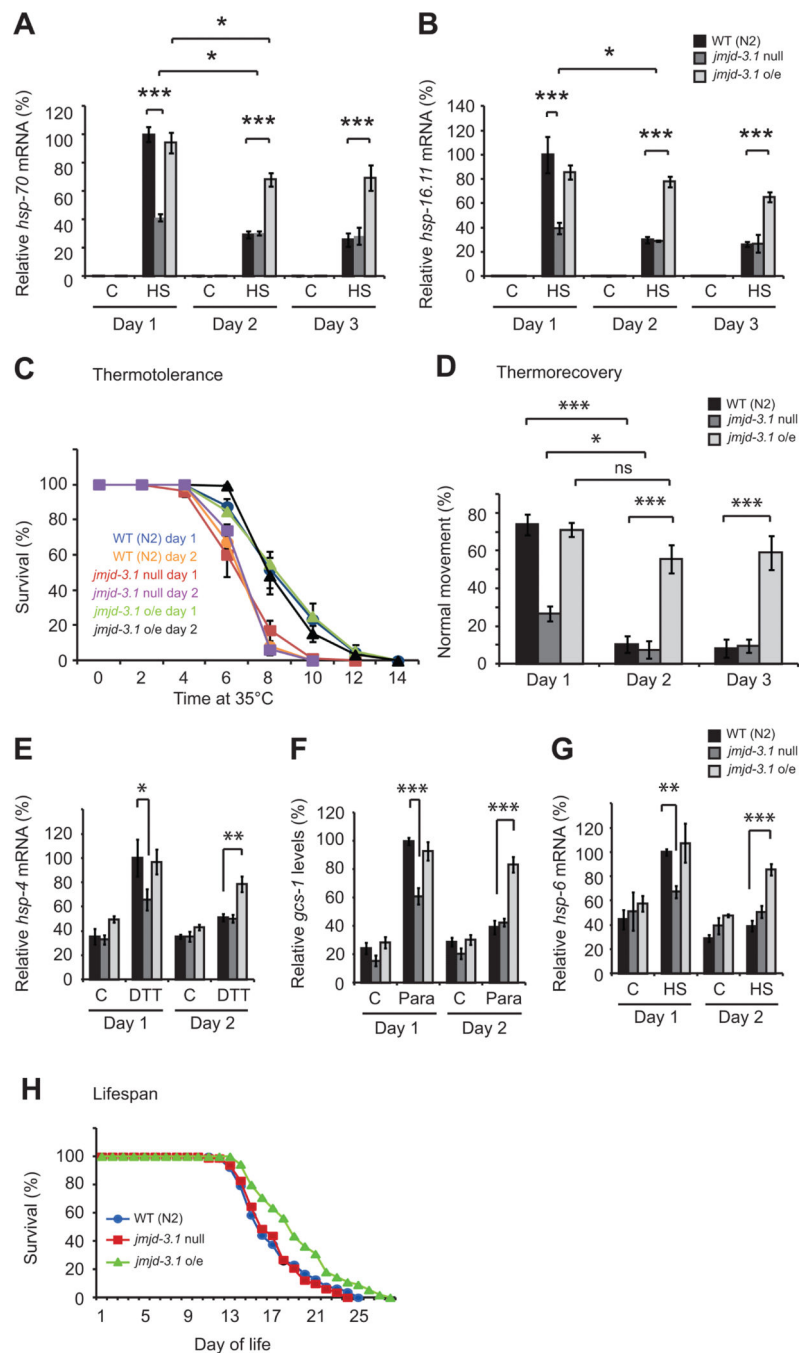


Figure 5. The timing of stress response decline and loss of stress resistance is controlled by *jmid-3.1*

(A) *hsp-70* (*C12C8.1*) and (B) *hsp-16.11* expression in wild type (WT), *jmid-3.1* null and *jmid-3.1* over-expressing (o/e) worms exposed to control (c) or HS (33°C, 30 min) conditions. (C) Survival of day 1/day 2 WT (blue/orange), *jmid-3.1* null (red/purple) and *jmid-3.1* o/e (green/black) worms at 35°C. Day 2 WT vs day 2 *jmid-3.1* oe, $p = 0.0022$; day 1 WT vs day 1 *jmid-3.1* null, $p = 0.0096$. (D) Thermorecovery of WT, *jmid-3.1* null and *jmid-3.1* o/e animals. (E) *hsp-4*, (F) *gcs-1* and (G) *hsp-6* expression in WT, *jmid-3.1* null

and *jmjd-3.1* o/e worms exposed to control (c) conditions, 33°C heat shock (HS) for 30 min or 200 mM paraquat (para) for 2 hours. **(H)** Lifespan analysis at 20°C. WT (blue line), *jmjd-3.1* null (red line) and *jmjd-3.1* o/e (green line). WT vs *jmjd-3.1* o/e, $p = 0.0006$. See table S1 and table S2 for all statistical comparisons. Values plotted are the mean of at least 4 independent experiments and bars represent SEM. Statistical significance was calculated by two-way ANOVA with Bonferroni post analysis comparison except in panel H where log-rank test was used. * $p < 0.05$, ** $p < 0.01$, *** $p < 0.001$. See also figure S5.

Author Manuscript

Author Manuscript

Author Manuscript

Author Manuscript

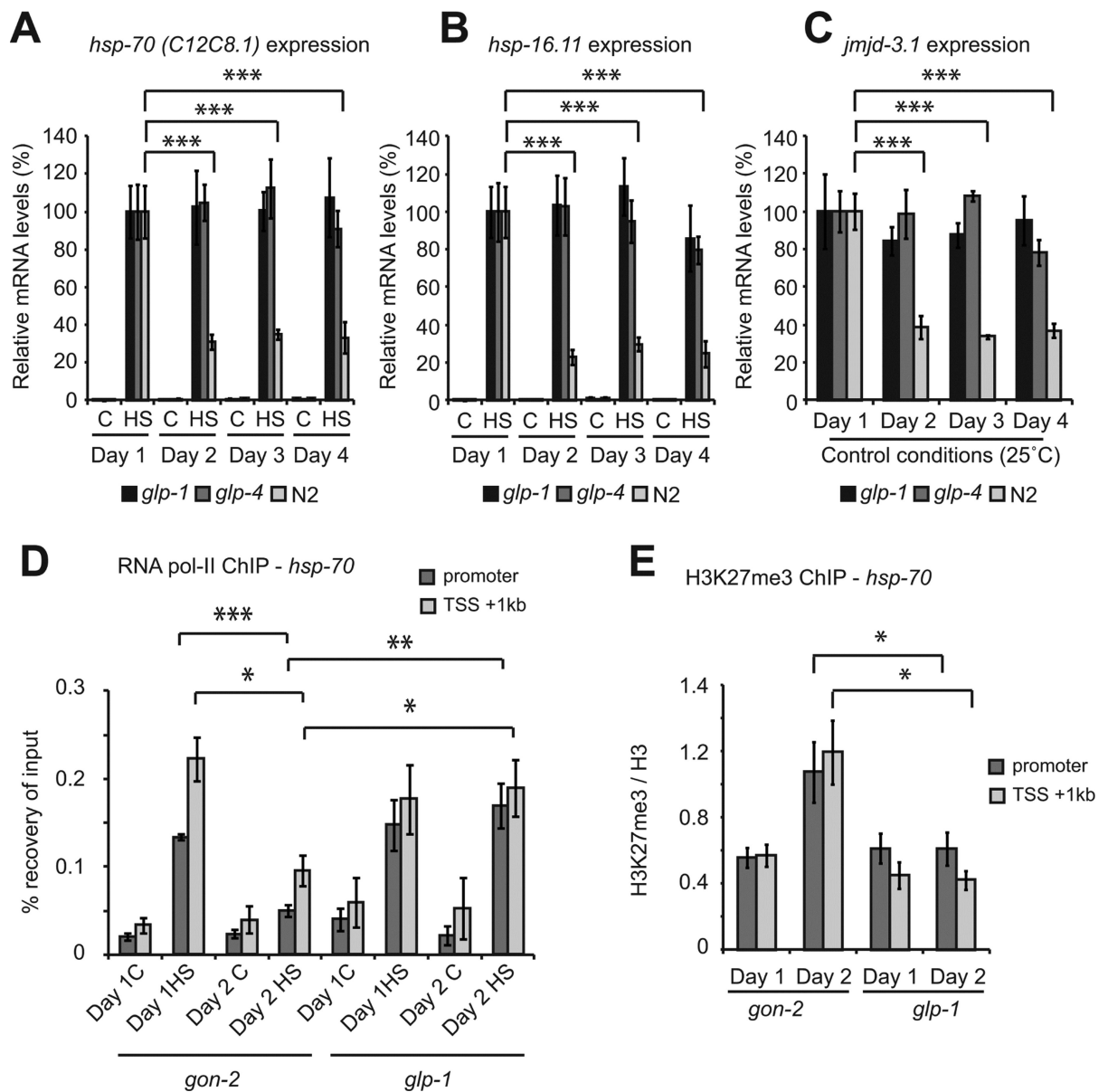


Figure 6. Removal of germ line stem cells maintains *jmjd-3.1* expression, suppresses accumulation of H3K27me3 and restores transcription at heat shock genes

Expression of (A) *hsp-70* (*C12C8.1*) and (B) *hsp-16.11* in wild type, *glp-1* (*e2141ts*) and *glp-4* (*bn2ts*) mutants maintained at 25°C and exposed to control (C) or heat shock (HS) conditions during early adulthood. (C) Expression of *jmjd-3.1* at different days of adulthood in wild type, *glp-1* and *glp-4* worms maintained at 25°C. (D) RNA pol-II (*ama-1*) or (E) H3K27me3 ChIP-qPCR in *gon-2* and *glp-1* animals maintained at 25°C. Values plotted are the mean of at least 4 biological replicates and error bars represent SEM. Statistical significance was calculated by one-way ANOVA (A-C) with Tukey post analysis comparison or two-way ANOVA with Bonferroni post analysis comparison (D and E). * $p < 0.05$, ** $p < 0.01$, *** $p < 0.001$. See also figure S6.

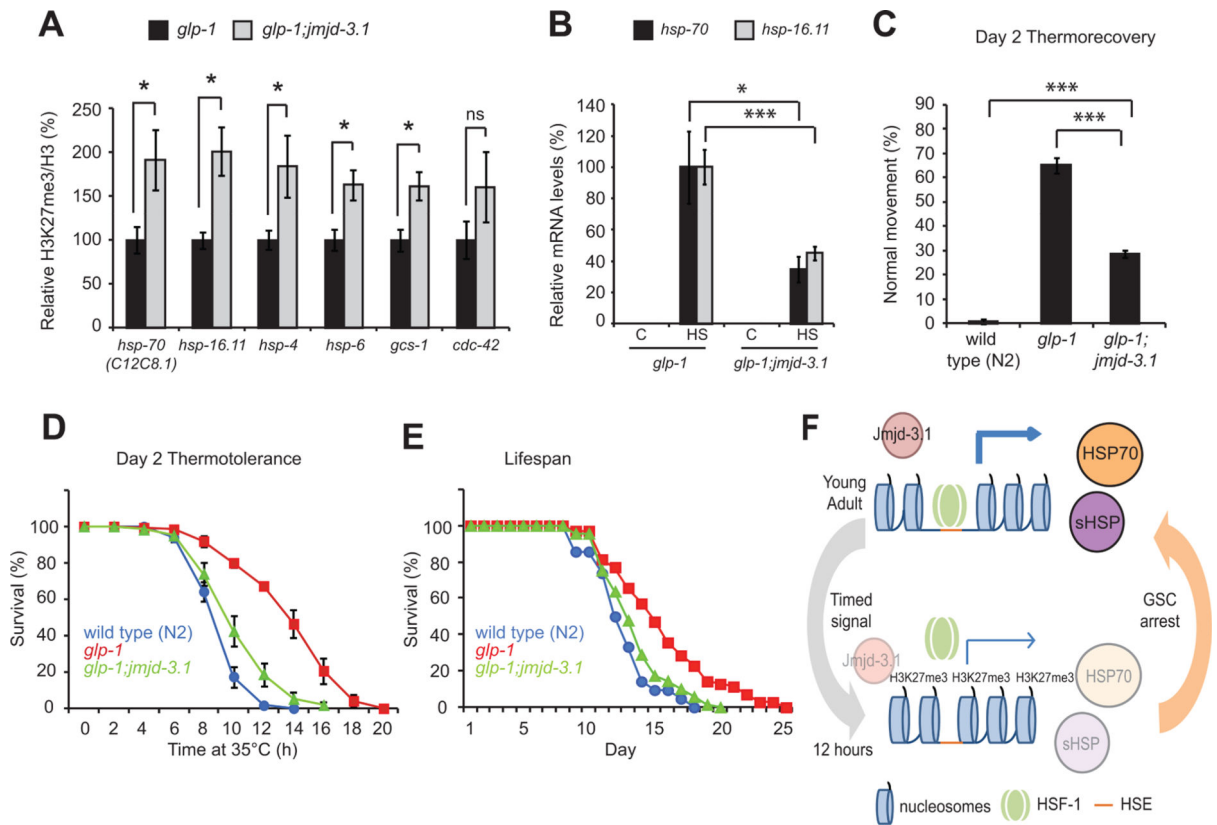


Figure 7. *glp-1* mutants maintain the HSR, enhance stress resistance and increase lifespan through *jmjd-3.1*

(A) ChIP-qPCR of H3K27me3 at stress gene loci in day 2 adult *glp-1(e2141ts)* and *glp-1(e2141ts);jmjd-3.1(gk384)* animals. (B) HS gene expression in *glp-1* and *glp-1;jmjd-3.1* double mutant animals exposed to control or heat shock conditions at day 2 of adulthood. (C) Thermorecovery (at day 2 of adulthood), (D) thermotolerance (at day 2 of adulthood) and (E) lifespan analysis of wild type (N2) (blue line), *glp-1* (red line) and *glp-1;jmjd-3.1* (green line) worms raised at 25°C. For (D): *glp-1* vs *glp-1;jmjd-3.1*, $p = 0.0013$; N2 vs *jmjd-3.1(gk384)*, $p = 0.081$. For (E): Mean lifespan in days were N2, 12.67 ± 0.35 ; *glp-1*, 15.61 ± 0.46 and *glp-1;jmjd-3.1*, 14.2 ± 0.28 ; *glp-1* vs *glp-1;jmjd-3.1(gk384)*, $p = 0.0001$. For all statistical comparisons see Tables S1 and S2. Values plotted are the mean of at least 3 independent experiments and error bars represent SEM. Statistical significance was calculated using Student's *t*-test (A and B), one-way ANOVA (C), two-way ANOVA (D) or log-rank test (E). * $p < 0.05$, ** $p < 0.01$, *** $p < 0.001$, ns $p > 0.05$. (F) Proposed model for programmed repression of the HSR. Thickness of blue arrows represents relative levels of transcription and intensity of circles represents relative protein levels. Cylinder (nucleosome) proximity represents chromatin accessibility. HSE = heat shock element, sHSP = small heat shock protein. See also figure S7.